

A STUDY ON THE ELECTRICAL DOUBLE LAYER THICKNESS IN MICRO CAPILLARIES

*School of Mechanical & Production Engineering,
Nanyang Technological University, Nanyang Ave, Singapore 639798*

Key words: Debye-Huckel length, zeta potential, electrical double layer.

1. Introduction

Micro channel technology has important applications in Bio-MEMS. An understanding of the microscopic transport phenomena in micro capillaries is vital to the design and process control of various fluidic devices. A survey of literature on micro channel research indicates that progress has been made steadily towards the understanding and the of micro channels behavior. These include, for examples, micro channels in a form of an infinite parallel plate [3] and rectangular micro channels [4, 5, 6]. The effects of the electrical potential on the liquid transport in a tiny cylindrical capillary have also been studied by Rice and Whitehead [7]. Their work is extended by Levine for developing micro transport models suitable for higher zeta potential [8]. Recently, Mala has indicated that, in micro scale flow, the interfacial electrokinetic effects associated with the electrical double layer (EDL) must be considered when the hydraulic radius of the flow channel is of comparable to the thickness of the EDL [3, 4].

Traditionally, the Debye-Huckel length has been used as a measure of the EDL thickness [1, 5]. There is however, reservation about this interpretation in micro capillaries. This is because Debye-Huckel length is originally derived to represent the effective size of ionic atmosphere for an ion, which gives an indication of the distance between the central ion and its surrounding charges in the ionic atmosphere. The EDL originating from the zeta potential at the solid-liquid interface in a micro capillary might have a different thickness. Hunter has suggested the EDL thickness at the solid-liquid interface is in the order of 3 to 4 times that of the traditional definition but no evidence was given. It is the objective of the present study to introduce a coefficient, which can be conveniently selected to define the region of EDL quantitatively. The study could be used to support Hunter's suggestion with theoretical ground.

2. The electrical double layer model

It is known that most of solid surfaces carry electrostatic charges, which give rise to an electrical surface potential. Electrical charges are also inevitably present in the liquid solution, for instance due to impurities or intentionally applied. The electrical charges on the solid surface will attract the counter-ions in the liquid. The arrangement of the charges on the solid surface and the balancing charges in the liquid is called the electrical double layer [1, 2]. Fig. 1 shows the structure of an EDL in accordance with the Gouy-Chapman theory with an excess of ions of opposite sign established on the wall. There are two layers in an EDL, a compact layer and a diffuse layer [1]. The separation boundary between these two layers is called the outer Helmholtz plane (OHP) where the diffusive layer begins and extends into the solution phase. The OHP is the plane of closest approach of ions in the solution and thus represents the effective location of the solid/liquid interface. The electrical potential at this plane is called the zeta potential, which characterizes the diffusive part of EDL. Comparing to the compact layer, the diffuse layer covers most of the EDL region and has a detrimental effect on micro capillary performance as well as on the behavior of solution. The compact layer is normally in the order of 0.5 nm thick [1, 2]. It is assumed to be a charge-free region where ions are strongly oriented and are confined to the wall surface. As a result, ions are immobile in the compact layer and are not able to react to an applied electric field.

In the diffuse layer, ions are affected by the local equilibrium of electrostatic potential and are mobile. The thickness of EDL mainly depends on the electrical potential of the solid surface, the bulk ionic concentration and the properties of the liquid. It ranges typically from tens of nanometers to several hundreds of nanometers [1, 2].

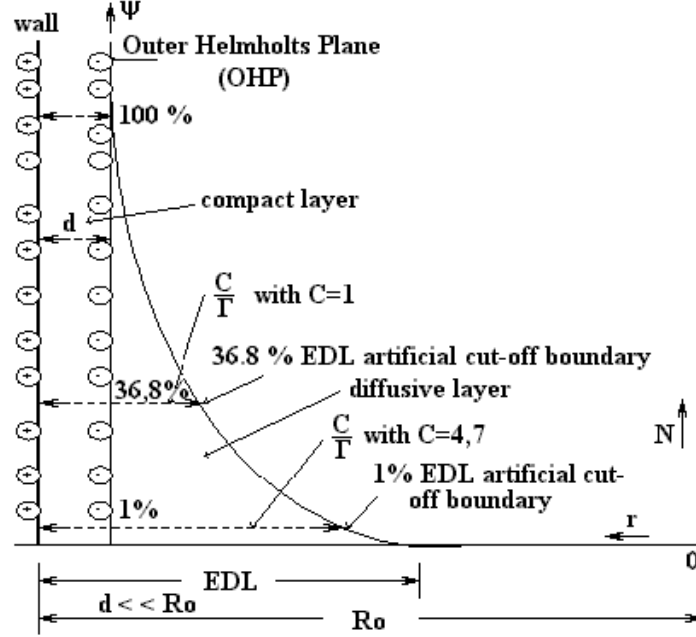


Fig. 1. The structure of an electrical double layer.

Zeta potential and EDL have close relation with respect to the distribution of net charge density in the solution. Consider a micro capillary of radius R_0 in cylindrical coordinate. Due to axis-symmetry of the circular geometry, the electrical potential can be assumed to vary in the radial r -direction and is uniform in the z -direction. The relationship between the electrical potential, ζ and the net charge density per unit volume, ρ_e at any point in the solution can be described by the Poisson equation as follows [1]:

$$\frac{1}{r} \frac{\partial}{\partial r} \left(r \frac{\partial \zeta}{\partial r} \right) = - \frac{\rho_e}{\varepsilon_r \varepsilon_0}, \quad (1)$$

where ε_r and ε_0 are the dielectric constant of the fluid and permittivity of vacuum. The number of ions per unit volume, n is assumed to be given by the Boltzmann distribution as follows [1]:

$$n = n_0 \exp\left(-\frac{Z_e e}{k_b T} \zeta\right), \quad (2)$$

where e and k_b are the electron charge and Boltzmann constant respectively. n_0 is the bulk concentration of ions per unit volume. T is the solution absolute temperature and Z_e is the valency of ion. The Boltzmann distribution is generally valid if the fluid flow in the micro capillaries has a very small Peclet number or in a fully developed hydrodynamic state [3]. The net charge density per unit volume is then given by the difference between symmetric cations and anions.

$$\rho_e = Z_e (n_+ - n_-) = -2Z_e n_0 \sinh\left(\frac{Z_e e \zeta}{k_b T}\right). \quad (3)$$

Substituting Eq. (3) into Eq. (1), the well-known Poisson-Boltzmann equation is obtained:

$$\frac{1}{r} \frac{\partial}{\partial r} \left(r \frac{\partial \zeta}{\partial r} \right) = \frac{2Z_e n_0}{\varepsilon \varepsilon_0} \sinh\left(\frac{Z_e e \zeta}{k_b T}\right). \quad (4)$$

By introducing the following non-dimensional groups together with the Debye-Huckel length,

$$R = \frac{r}{D_0}, \Psi = \frac{Z_e e \zeta}{k_b T}, \Gamma = D_0 K,$$

where $K = \sqrt{\frac{2Z_e^2 e^2 n_0}{\epsilon_r \epsilon_0 k_b T}}$ and Γ are the Debye-Huckel length and the non-dimensional Debye-Huckel length respectively. D_0 is the capillary diameter.

Eq. (4) can be written in non-dimensional form as:

$$\frac{1}{R} \frac{\partial}{\partial R} \left(R \frac{\partial \Psi}{\partial R} \right) = \Gamma^2 \sinh \Psi. \quad (5)$$

The reciprocal of Debye-Huckel length ($1/K$) is normally referred to as the thickness of the electrical double layer. It describes the effect due to spatial variation of charge distribution originated from the zeta potential. It is assumed that the zeta potential is small as compared to the thermal energy of the ions in the solution, i.e.,

$$|Z_e e \zeta| < k_b T, \text{ and thus } \zeta < 0.01V, \text{ with } Z_e = 2.$$

This is generally valid for low concentration solutions in which diffusion transport is of secondary important. This approach is known as the Debye-Huckel approximation with which the electrical potential governing equation can be simplified as:

$$\frac{1}{R} \frac{\partial}{\partial R} \left(R \frac{\partial \Psi}{\partial R} \right) = \Gamma^2 \Psi \approx \Gamma^2 \sinh \Psi. \quad (6)$$

Consider axis-symmetry and that the compact layer is much thinner than the effective EDL thickness, i.e. $d \ll \text{Effective EDL thickness} < R_0$. The following boundary conditions are specified:

$$\text{At the center, } R = 0, \frac{\partial \Psi}{\partial R} = 0.$$

$$\text{At the outer Helmholtz plane, } R = \frac{R_0 - d}{D_0} \approx \frac{1}{2}, \Psi = \zeta_0^0.$$

where d and R_0 are the compact layer thickness and capillary radius respectively. The non-dimensional zeta potential is defined as: $\zeta_0^0 = \frac{Z_e e \zeta_0}{k_b T}$, where ζ_0 is the zeta potential at the OHP boundary.

The electrical potential distribution along the capillary radius can be obtained by solving the above governing equation using the power series method. Assuming the solution can be represented by a power series of the following form:

$$\Psi = \sum_{n=0}^{\infty} a_n R^n,$$

the following solution is obtained:

$$\Psi = \frac{\zeta_0^0 \sum_{n=0}^{\infty} \frac{\Gamma^{2n}}{2^{2n} (n!)^2} R^{2n}}{\sum_{n=0}^{\infty} \frac{\Gamma^{2n}}{2^{4n} (n!)^2}}. \quad (7)$$

The above can be written in terms of the relative electrical potential, ψ defined as:

$$\psi = \frac{\Psi}{\zeta_0^0} = \frac{F(IR)}{F(\frac{\Gamma}{2})}, \quad (8)$$

where

$$F(IR) = \sum_{n=0}^{\infty} \frac{\Gamma^{2n}}{2^{2n} (n!)^2} R^{2n} .$$

3. Results and analyses

3.1. The effects of non-dimensional Debye-Huckel length

It can be seen from the EDL model that the non-dimensional Debye-Huckel length, Γ is an important parameter controlling the electrical potential distribution in the solution and is of influential to the performance of the micro capillaries. Based on Eq. (8), the relationship between the relative electrical potential and the non-dimensional radius for various values of Γ is shown in Fig. 2. It can be found that the electrical potential decreases rapidly in the region close to the capillary wall. As Γ increases, the spatial rate of change of electrical potential also increases and the EDL boundary is getting closer and closer to the wall. The charge density per unit area at the interface will also increase since it is proportional to the electrical potential gradient. As the EDL region is reduced, the effects of EDL are expected to diminish. Such a process is generally referred to as compression of EDL. Thus, from the capillary operation and performance point of view, a large Γ is desirable to suppress the electro-kinetic effects.

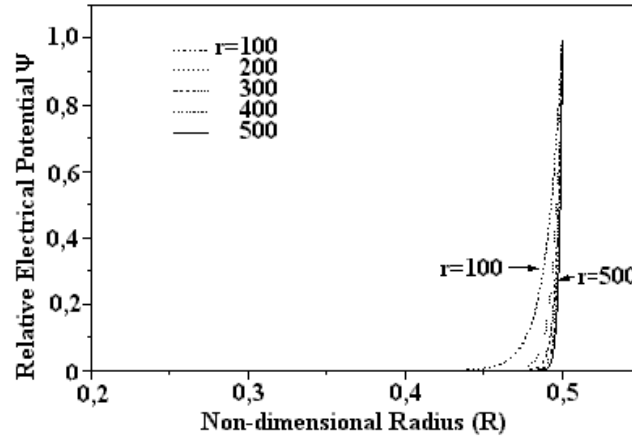


Fig. 2. The distribution of relative electrical potential along radial direction for various non-dimensional D-H length.

The non-dimensional Debye-Huckel length also describes the relation between the solution concentration and capillary size as depicted by the following expression:

$$\Gamma = D_0 \sqrt{\frac{2Z_e^2 e^2 \eta N_a}{k_b T}} , \quad (9)$$

where N_a is the Avogadro number.

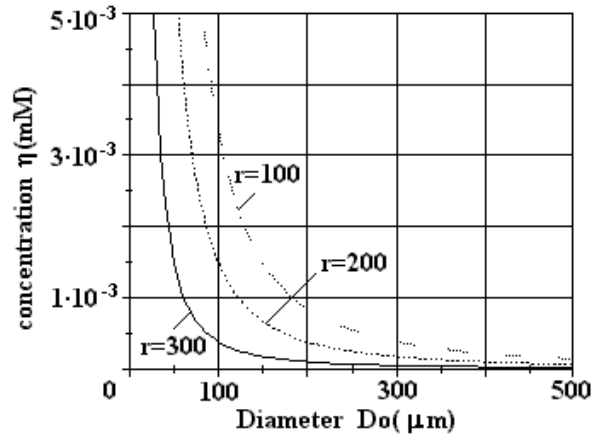


Fig. 3. Relation between tube diameter and solution concentration for various non-dimensional D-H length.

This relationship is illustrated in Fig. 3. This figure provides useful information in the design/selection of capillary size and solution concentration to meet with the requirements set by the non-dimensional Debye-Huckel length. This will help to warrant the capillary performance as the electro-kinetic effects are suppressed when a large Γ can be implemented.

3.2. The effects of capillary diameter

Assuming low concentration, e.g. $\eta=1.0e-3$ (mM), Fig. 4 shows the relative electrical potential distribution along the capillary radius as the diameter changes from 10 μm to 100 μm .

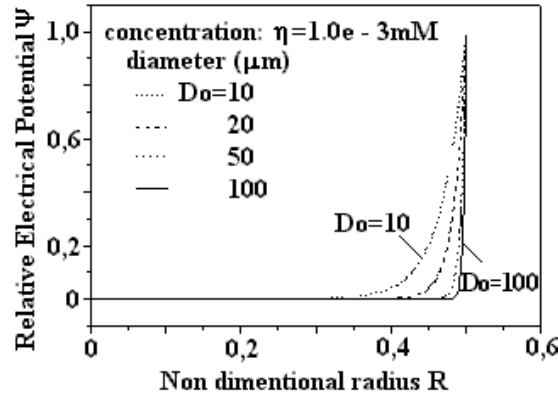


Fig. 4. Relative electrical potential distribution along tube radius as a function of diameter.

Similar to Fig. 2, Fig. 4 also shows a rapid variation of relative electrical potential near the capillary wall. For a given solution concentration, the electrical potential changes rapidly as the diameter increases and is confined within a very thin layer. It also can be observed from the same figure that the electrical potential is influential to the micro capillary performance when the capillary diameter is getting smaller ($<20 \mu\text{m}$). For example, the EDL region covers about 30% of the capillary radius when $D_0 = 10 \mu\text{m}$ and $\eta=1.0e-3$ (mM). This observation agrees with the Mala's finding that electrokinetic effects must be considered when the tube sizes reduce to this order of magnitude [3, 4].

3.3. The effects of solution concentration

Assuming a fixed capillary diameter, e.g. $D_0 = 50 \mu\text{m}$, the relative electrical potential distribution along the radius is shown in Fig. 5 with solution concentration varies from $1.0e-4$ (mM) to $2.0e-3$ (mM).

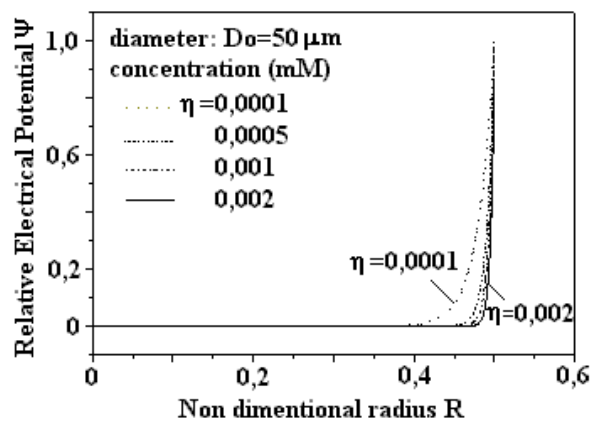


Fig. 5. Relative electrical potential distribution along the capillary radius at various concentration levels.

From Fig. 5, it is noted that the relative electrical potential also varies greatly near the capillary wall. For a given capillary diameter, with higher concentration, the greater the spatial rate of change of electrical potential occurs and the EDL is closer to the wall. This also leads to compression of EDL. On the other hand, when the solution concentration is getting lower (< 0.0001 mM), the electrical potential in the EDL becomes influential to the micro capillary performance and the behavior of the solution. This observation agrees with the results from other researchers [1, 2, 3, 4].

From the above results, it can be said that the rapid change of electrical potential near the capillary wall is a unique feature of the interfacial phenomenon in micro capillaries. This reveals strong interaction at the solid/liquid interface.

4. Assessment of EDL thickness

Traditionally, the thickness of EDL is characterized by the reciprocal of Debye-Huckel length, which can be expressed as $\frac{1}{\Gamma}$ in non-dimensional form. This parameter has been generally used as a measure of EDL thickness. Because the compact layer is much thinner than that of the diffuse layer, $\frac{1}{\Gamma}$ represents mainly the thickness of the diffuse layer. However, this is not an adequate representation of the effective thickness of EDL because the zeta potential does require a finite distance to decrease its value to that of the solution. These phenomena have been depicted in Figs. 2, 4 and 5 inclusively. For examples, the relative electrical potential is equal to 36.8% of its maximum value if the thickness of EDL is considered to be $\frac{1}{\Gamma}$. When the relative electrical potential equals to 5% of its maximum value, the thickness of EDL will extend to three times of $\frac{1}{\Gamma}$ (or $\frac{3}{\Gamma}$). Therefore, $\frac{1}{\Gamma}$ covers only a small portion of the EDL region. It is necessary to introduce a numerical coefficient, C to extend the traditional EDL thickness from $\frac{1}{\Gamma}$ to $\frac{C}{\Gamma}$.

By applying Eq. (8) at the outer Helmholtz plane, located at $R = 0.5 - \frac{C}{\Gamma}$, and selecting a specific value of interest for the relative electrical potential at this artificial cut-off boundary, one has:

$$\psi \Big|_{\substack{\text{@ cut-off} \\ \text{boundary}}} = \frac{\Psi}{\zeta_0} = \left[\frac{F(IR)}{F(\frac{\Gamma}{2})} \right] \Big|_{R=0.5-C/\Gamma} = \begin{cases} 1\% \\ 0.5\% \\ 0.1\% \\ 0.05\% \\ 0.01\% \end{cases} \quad (10)$$

For a given relative electrical potential at cut-off boundary, the above expresses the relation between the coefficient C and Γ and is depicted in Fig. 6.

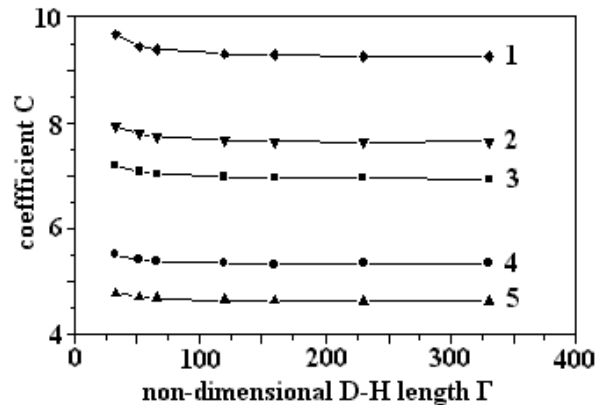


Fig. 6. Variation of coefficient C with non-dimensional $D-H$ length at different relative electrical potential: 1 – $\eta=0,01\%$; 2 – $0,05\%$; 3 – $0,1\%$; 4 – $0,5\%$; 5 – 1% .

It can be found from Fig. 6 that the coefficient C depends on the relative electrical potential selected at the cut-off boundary but is independent of the non-dimension $D-H$ length. It is also of interesting to examine the relationship between the coefficient C and the tube diameters as well as the solution concentration. These are shown in Figs. 7 and 8 respectively. The coefficient C remains unaltered no matter what value of the capillary diameter or the solution concentration is chosen. In this respect, the coefficient can be regarded as a universal constant, which defines the effective EDL thickness when the relative electrical potential at cut-off boundary is chosen.

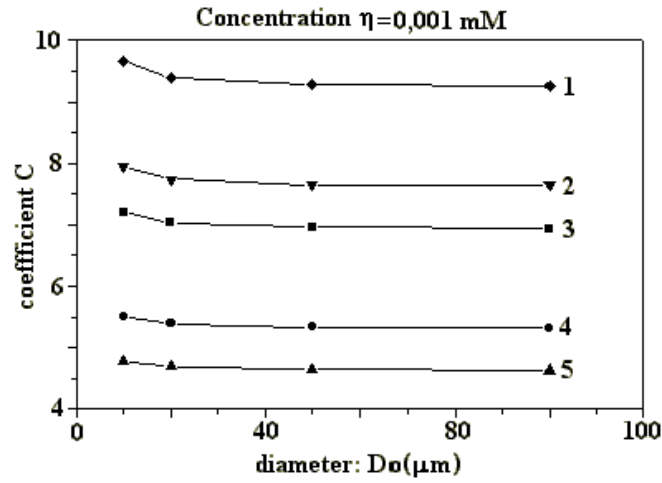


Fig. 7. Variation of coefficient C with capillary diameter at different relative electrical potential ($\eta=0,001$ mM): 1 – $\psi=0,01\%$; 2 – $0,05\%$; 3 – $0,1\%$; 4 – $0,5\%$; 5 – 1% .

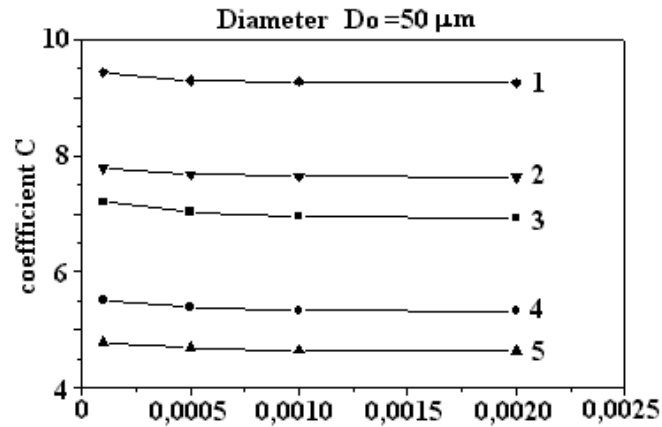


Fig. 8. Variation of coefficient C with solution concentration at different relative electrical potential ($D_0 = 50$ μm): 1 – $\psi=0,01\%$; 2 – $0,05\%$; 3 – $0,1\%$; 4 – $0,5\%$; 5 – 1% .

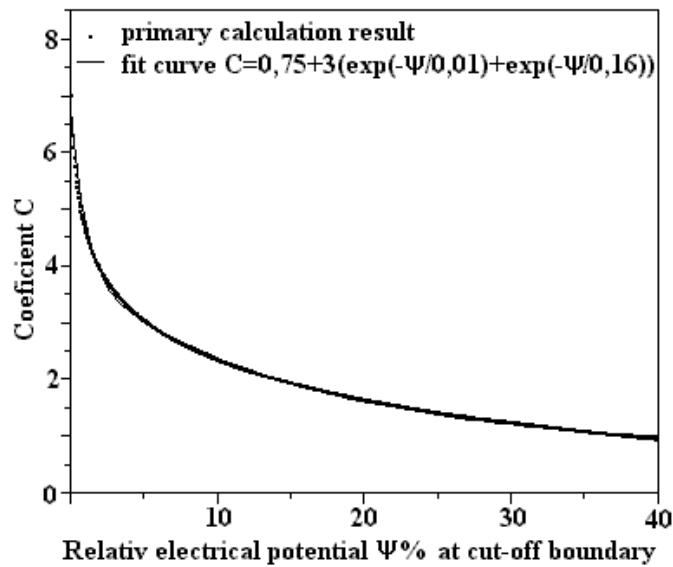


Fig. 9. Variation of coefficient C with the relative electrical potential at EDL cut-off boundary.

Fig. 9 shows the coefficient C as a function of the relative electrical potential at cut-off boundary. C increases as the electrical potential at EDL boundary cut-off is reduced. In general, the coefficient C can be determined by the following expression, which is obtained by curve-fit from Fig. 9.

$$C = 0,75 + 3e^{-\frac{\Psi_{cut-off}}{0,01}} + 3e^{-\frac{\Psi_{cut-off}}{0,16}} . \quad (11)$$

The EDL boundary can be conveniently defined by selecting a suitable relative electrical potential at the cut-off point. This is an artificial boundary separating the EDL from the solution. With reference to Fig. 9, it is suggested to apply 1% relative electrical potential as the cut-off boundary. This yields $C = 4.7$ for 1% cut-off. The effective thickness of EDL is about 4.7 times bigger than the traditional value, which corresponds to $C = 1$. Table 1 shows a comparison of the EDL cut-off point between the newly defined EDL effective thickness and the traditional one. The same is also illustrated graphically in Fig. 1. The 36.8% of relative electrical potential as the cut-off boundary for the traditional thickness are too high to be acceptable. This does not appear to be an adequate representation of the effective EDL thickness. Instead, the tradition thickness should be interpreted as the characteristic thickness of EDL. Hunter has suggested that the EDL region extends to the order of $3/K \sim 4/K$ from the wall [1, 2]. This corresponds to $C = 3$ or $C = 4$ and is in close agreement with the present study ($C = 4.7$).

Table 1. Comparison of effective EDL thickness and traditional one

	Effective thickness $C = 4.7$		Tradition thickness $C = 1$	
	$\Gamma=100$	$\Gamma=200$	$\Gamma=100$	$\Gamma=200$
$\left. \frac{1}{\zeta_0^0} \frac{\partial \Psi}{\partial R} \right _{0,5-\frac{C}{\Gamma}}$	0.95	1.85	36.8	73.6
$\left. \Psi = \frac{\Psi}{\zeta_0^0} \right _{0,5-\frac{C}{\Gamma}}$	1%		36.8%	

As an example, consider a capillary diameter, $D_0 = 50 \mu\text{m}$, solution concentration $\eta = 0.001 \text{ mM}$ and at a temperature of 298 K. This leads to $K = 3.2 \mu\text{m}^{-1}$ and $\Gamma = 160$. The non-dimensional EDL effective thickness can also be expressed as:

$$\frac{\text{Effective EDL thickness}}{R_0} = \frac{2C}{\Gamma} . \quad (12)$$

From above, the non-dimensional traditional EDL thickness and effective EDL thickness will be equal to 0.006, with $C = 1$ and 0.029, with $C = 4.7$ respectively. Based on 1% relative electrical potential cut-off, the effective EDL thickness will cover 5.8% of the capillary radius. That is to say one is able to limit the effects of EDL within 5.8% of the capillary radius. This shows that the non-dimensional Debye-Huckel length is indeed a parameter of prominent significance in EDL theory as well as in the practical operation of micro capillaries.

5. Conclusion

The study shows that the distribution of electrical potential in the EDL is mainly determined by the non-dimensional Debye-Huckel length, Γ . A suitable value of Γ can be chosen to limit the effects of EDL. This aids in selecting a suitable capillary diameter and solution concentration to warrant the capillary performance.

The EDL thickness and the effects of EDL at the solid-liquid interface are also analyzed in this work. A coefficient C , being independent of Γ , is introduced to define the effective EDL thickness. It is suggested to apply 1% relative electrical potential as the cut-off point for the EDL boundary giving rise to a value of $C = 4.7$. The results show that the effective EDL thickness is 4.7 times greater than that of the traditional definition and are in close agreement with Hunter's suggestion (3~4).

The study reveals that the tradition EDL thickness corresponds to $C = 1$. It is suggested to interpret it as the characteristic thickness of EDL.

Appendix

Series solution to the potential

In simplified two dimension modeling, zeta potential can be expressed as:

$$\frac{1}{R} \frac{\partial}{\partial R} \left(R \frac{\partial \Psi}{\partial R} \right) = \Gamma^2 \Psi. \quad (9)$$

Boundary conditions:

$$\text{at } R = 0 \quad \frac{\partial \Psi}{\partial R} = 0, \quad \text{and} \quad R = \frac{R_0}{D_h}, \quad \Psi = \zeta_0^0.$$

By defining:

$$\Psi = \sum_{n=0}^{\infty} a_n R^n \quad (10)$$

following equations can be developed:

$$\frac{\partial \Psi}{\partial R} = \sum_{n=0}^{\infty} (n+1) a_{n+1} R^n;$$

$$\frac{1}{R} \frac{\partial \Psi}{\partial R} = \frac{a_1}{R} + \sum_{n=0}^{\infty} (n+2) a_{n+2} R^n;$$

$$\frac{\partial^2 \Psi}{\partial R^2} = \sum_{n=0}^{\infty} (n+1)(n+2) a_{n+2} R^n.$$

Equation(1) can then be written in series as:

$$\sum_{n=0}^{\infty} (n+1)(n+2) a_{n+2} R^n + \frac{a_1}{R} + \sum_{n=0}^{\infty} (n+2) a_{n+2} R^n = \sum_{n=0}^{\infty} \Gamma^2 a_n R^n. \quad (11)$$

From equation (22) coefficient can be obtained:

$$a_1 = 0;$$

$$(n+1)(n+2) a_{n+2} + (n+2) a_{n+2} = \Gamma^2 a_n$$

then coefficient can be expressed as

$$a_{2n} = \frac{\Gamma^{2n}}{2^{2n} (n!)^2} a_0, \quad \text{and} \quad a_{2n+1} = 0.$$

Using above coefficient expression, equation(21) can be written as

$$\Psi = \sum_{n=0}^{\infty} \frac{\Gamma^{2n}}{2^{2n} (n!)^2} a_0 R^{2n}. \quad (12)$$

Considering that $D_0 \ll L$, $\frac{R_0}{D_h} = \frac{1}{2}$. According to the boundary conditions, coefficient a_0 can be obtained

$$a_0 = \frac{\zeta_0^0}{\sum_{n=0}^{\infty} \left(\frac{\Gamma^{2n}}{2^{4n} (n!)^{2n}} \right)}$$

By defining

$$F(\Gamma R) = \sum_{n=0}^{\infty} \frac{\Gamma^{2n}}{2^{2n} (n!)^2} R^{2n}$$

zeta potential equation(7) will be written as:

$$\Psi = \frac{F(\Gamma R)}{F\left(\frac{\Gamma}{2}\right)} \zeta_0^0 \quad (13)$$

Above given the whole zeta potential series expression.

Considering a fully developed flow of an aqueous 1:1 electrolyte (the KCl solution) through the capillary, the following parameters can be obtained in table 2.

Table 2

<i>Relevant parameters</i>		
Parameter	Value	Description
k_b	1.38e-23(J K ⁻¹)	Boltzmann constant
ϵ_0	8.85e-12(C ² N ⁻¹ m ⁻²)	permittivity of vacuum
Z_e	1	number of the valence of ions
E	1.60e-19(C)	electron charge
T	298(K)	absolute temperature
ϵ	78.5	dielectric constant of solution

Nomenclature

a_n	power series coefficient
d	distance of OHP plane from the tube wall (m)
D_0	capillary diameter (m)
e	electron charge (C)
k_b	Boltzmann constant (1.38×10 ²³ J K ⁻¹)
K	Debye-Huckel length ($\kappa = \sqrt{\frac{2Z_e^2 e^2 n_0}{\epsilon \epsilon_0 k_b T}}$) (m ⁻¹)
n	number of ions per unit volume (m ⁻³)
n_0	bulk concentration of ions per unit volume (m ⁻³)
N_a	Avogadro number
R_0	capillary radius (m)
R	non-dimensional radius
T	solution absolute temperature (K)
Z_e	valency of ion
r, θ, z	cylindrical coordinate (r, θ and z)

Greek symbols

η	bulk solution concentration (mM)
ρ_e	net electric charge density per unit volume on channel wall (C m^{-3})
ζ	electrical potential (V)
ζ_0	zeta potential at the OHP boundary between the diffuse layer and the compact layer (V)
ζ_0^0	non-dimensional zeta potential ($\zeta_0^0 = \frac{Z e \zeta_0}{k_b T}$)
Ψ	non-dimensional electrical potential
ψ	relative electrical potential ($\psi = \Psi / \zeta_0^0$)
ε_r	dielectric constant of the fluid
ε_0	permittivity of vacuum ($8.85 \times 10^{-12} \text{C V}^{-1} \text{m}^{-1}$)
Γ	non-dimensional Debye-Huckel length ($\Gamma = D_0 K$)

REFERENCES

1. *Hunter R.J.* Foundations of colloid science, Vol. I & II, Oxford Science Publication, 1993.
2. *Hunter R.J.* Zeta potential in colloid science: principles and applications, Academic press, New York, 1981.
3. *Mala G.M., Li D., Werner C., Jacobasch H.J.* Flow characteristic of water through a microchannel between two parallel plates with electrokinetic effects // *International Journal of Heat and Fluid Flow.* 1997. Vol. 18. P. 489–496.
4. *Mala G.M., Li D., Dale J.D.* Heat transfer and fluid flow in microchannels // *International Journal of Heat and Mass Transfer.* 1997. Vol. 40. No.13. P. 3079–3088.
5. *Yang C., Li D., Masliyah J.H.* Modeling forced liquid convection in rectangular microchannels with electrokinetic effects // *International Journal of Heat and Mass Transfer.* 1998. Vol. 41. P. 4229–4249.
6. *Peng X.F., Peterson G.P., Wang B.X.* Heat transfer characteristics of water flowing through microchannels // *Experimental Heat Transfer.* 1994. No. 7. P. 265–283.
7. *Rice C.L., Whitehead R.* Electrokinetic flow in narrow cylindrical capillaries // *Journal of physical chemistry.* 1965. Vol. 69. P. 4017–4023.
8. *Levine S., Marriott J.R., Neale G., Epstein N.* Theory of electrokinetic flow in fine cylindrical capillaries at high zeta potentials // *Journal of colloid and interface science.* 1975. Vol. 52. P. 136–149.

Received 25.09.2000

Summary

The thickness and the effects of electrical double layer on micro capillaries are analyzed in the present study. The distribution of the electric potential in the double layer is first determined by solving the Poisson-Boltzmann equation in cylindrical coordinates using the power series method. A definition for the double layer effective thickness is introduced based on 1% relative electrical potential at the artificial cut-off boundary. In this approach, a coefficient, being independent of the non-dimensional Debye-Huckel length, is introduced and is applied successfully to assess the double layer effective thickness at the solid-liquid interface. The results show that the double layer effective thickness is 4.7 times greater than that of the traditional value based on the thickness of the ionic atmosphere at the ion-liquid interface. The results appear to be in close agreement with Hunter's suggestion. Example is also given to illustrate the applications of the present study.